E-ISSN 2586-9027
Homepage : https://tci-thaijo.org/index.php/SciTechAsia
Science & Technology Asia
Vol.31 No.3 July - September 2026
Page: [345-362]
Original research article

A Network Pharmacology Approach to Explore Flavonol Compounds from the KNApSAcK Database as Therapeutic Candidates for COVID-19

Neni Frimayanti*, Adriani Susanty, Uci Rahmadhanty

Sekolah Tinggi Ilmu Farmasi Riau, Jln Kamboja Panam, Pekanbaru 28293 Indonesia

Received 28 December 2025; Received in revised form 20 August 2026
Accepted 1 September 2026; Available online 30 September 2026

ABSTRACT

COVID-19 is an infectious disease caused by SARS-CoV-2. The identification of new therapeutic candidates targeting multiple proteins and biological pathways may provide an alternative strategy for COVID-19 treatment. This study aimed to investigate the potential of flavonol compounds as multitarget antiviral candidates against COVID-19 using network pharmacology and molecular docking approaches. Flavonol compounds were obtained from the KNApSAcK database and evaluated for drug-likeness based on Lipinski's Rule of Five using SwissADME. Flavonol-associated protein targets were predicted using SwissTargetPrediction, while COVID-19-related proteins were identified using GeneCards. The overlapping proteins were analyzed using a Venn diagram, followed by protein-protein interaction analysis using STRING-DB to identify potential hub proteins. Of the 25 flavonol compounds evaluated, 21 fulfilled the Lipinski criteria and were retained for further analysis. Network analysis identified 170 overlapping proteins and 16 hub proteins, comprising ACE2, ACE, AGT, REN, TMPRSS2, FURIN, CD4, CD8A, IL6, IL1B, IL10, TNF, IFNG, CRP, CXCL8, and CXCL10. ACE2 showed the highest connectivity and was therefore selected as a representative hub target for molecular docking. Based on docking binding free energy, the four flavonols with the most favorable predicted binding affinities toward ACE2 were Broussonol E, 5,7,3′,4′-tetrahydroxy-6-geranylflavonol, Broussoflavonol A, and Broussoflavonol B, all stronger than baicalein and sharing several interaction residues with the reference compound. These findings support the potential of the investigated flavonols as multitarget antiviral candidates at the network level, involving proteins associated with viral entry, the renin–angiotensin system, and immune and inflammatory responses. However, the present docking analysis provides target-specific structural

***Corresponding author:** nenifrimayanti@stifar-riau.ac.id doi.org/10.70730/sta.v31i3.263034

evidence only for ACE2. Further computational and experimental studies involving the remaining hub proteins are required to validate the proposed multitarget mechanism and antiviral activity.

Keywords: COVID-19; Flavonols; Network pharmacology; Molecular docking; SARS-CoV-2

1. Introduction

COVID-19, caused by the novel coronavirus SARS-CoV-2, first appeared in Wuhan, China, in late 2019 and quickly escalated into a global health crisis. The virus spreads mainly through respiratory droplets and direct contact, infecting the respiratory tract and often leading to fever, cough, and difficulty breathing. In severe cases, the infection can progress to pneumonia, acute respiratory distress, organ failure, or even death. Among the viral proteins, the spike protein is particularly important because it allows the virus to enter host cells, making it a critical target for therapeutic intervention [1, 2].

Despite progress in vaccine development and supportive therapies, the search for safe and effective antiviral agents remains urgent. Natural compounds are of particular interest because they often exhibit broad biological activities with fewer side effects. Flavonols are well-known for their antioxidant, anti-inflammatory, and antiviral properties [3-5]. Recent studies have shown that flavonols can block key viral proteins of SARS-CoV-2, including the spike protein, main protease (Mpro), and RNA-dependent RNA polymerase (RdRp), and compounds such as quercetin, fisetin, and myricetin have emerged as promising candidates [6-8]. These flavonols exert their antiviral effects through distinct but overlapping mechanisms. Quercetin, for example, has been shown to bind competitively within the active site of Mpro and to interfere with the interaction between the viral spike protein and the human ACE2 receptor, thereby blocking both viral replication and cell entry [8]. A comparative in vitro screening further demonstrated that commercially available flavonols exhibited stronger SARS-CoV-2 inhibitory activity than isoflavones and flavones, highlighting the importance of the flavonol scaffold itself for antiviral potency [7]. Beyond single-target inhibition, flavonols have also been reported to act as multitarget antivirals, showing binding affinity toward the main protease (3CLpro), papain-like protease (PLpro), the spike protein, RdRp, and ACE2 simultaneously [17]. Building on this evidence, a recent in silico study on a dimethoxy-substituted flavonol derivative reported favorable binding energy and key residue interactions with Mpro, supporting the flavonol scaffold as a promising and chemically tractable starting point for structure-based antiviral design [16]. Taken together, these findings indicate that flavonols are a mechanistically diverse, multitarget class of natural antivirals against SARS-CoV-2, providing the rationale for the present study, which expands on this evidence by systematically screening a wider panel of flavonol compounds through an integrated network pharmacology and molecular docking approach.

Modern drug discovery has also begun to embrace network pharmacology, a systems-level approach that examines how compounds interact with multiple biological targets rather than a single protein. When combined with molecular docking, this method can offer deeper insights into the mechanisms of action of potential drug candidates across complex biological networks [9]. This is a cost-effective and efficient method for uncovering new therapeutic strategies [10].

In this study, we applied network pharmacology and molecular docking to explore flavonol compounds from the KNApSAcK database as potential

multitarget antiviral agents against SARS-CoV-2. By mapping flavonol-associated proteins onto COVID-19-related proteins and identifying highly connected hub proteins, we aimed to provide evidence for the potential multitarget activity of flavonols at the systems level. Molecular docking was subsequently used to investigate ACE2, which showed the highest connectivity among the identified hub proteins, as a representative target. This study therefore distinguishes the network-level multitarget potential of the flavonol compounds from the target-specific structural evidence obtained by docking. The findings may contribute to understanding how natural flavonols could modulate multiple biological processes relevant to COVID-19 and provide a basis for further target-specific validation.

2. Materials and Methods

2.1 Compound collection and preparation

Flavonol compounds were obtained from the KNApSAcK database [14], which is a widely used source of plant secondary metabolites. A total of 20 flavonols were selected for analysis, with baicalein as a reference compound. The molecular structures were either obtained directly from the database or redrawn using ChemDraw Professional 15.0, followed by energy minimization in MOE 2022.02 using the MMFF94x force field to ensure stable conformations. A list of the compounds is presented in Fig. 1.

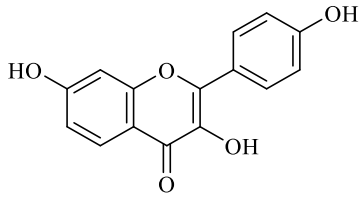
2.2 Protein target preparation

The structure of angiotensin-converting enzyme 2 (ACE2, PDB ID: 7BZ5) [20], a known entry receptor for SARS-CoV-2, was downloaded from the Protein Data Bank. To prepare the protein for docking, water molecules and bound ligands were removed using BIOVIA Discovery Studio Visualizer (DSV 2020), and the structure was refined using MOE 2022.02.

2.3 ADMET screening

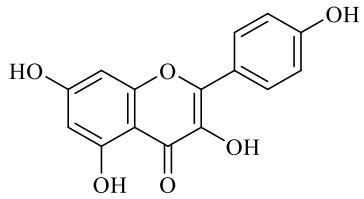
All 25 compounds were evaluated for pharmacokinetic suitability using SwissADME. The predictions focused on absorption, solubility, lipophilicity, and bioavailability. Compounds that satisfied Lipinski's Rule of Five (molecular weight <500, logP <5, hydrogen bond donors <5, hydrogen bond acceptors <10, with minimal violations) were prioritized for further studies [21,11].

SF2



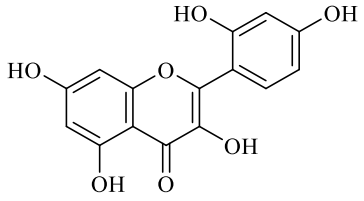
3,7-dihydroxy-2-(4-hydroxyphenyl)-4H-chromen-4-one

SF3



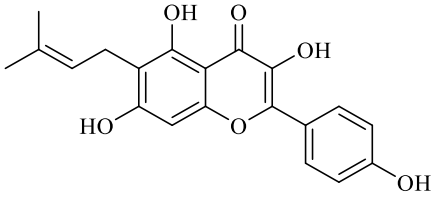
3,5,7-trihydroxy-2-(4-hydroxyphenyl)-4H-chromen-4-one

SF4



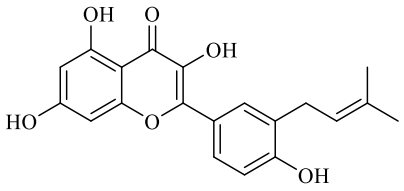
2-(2,4-dihydroxyphenyl-3,5,7- trihydroxy-4H-chromen-4-one

SF5



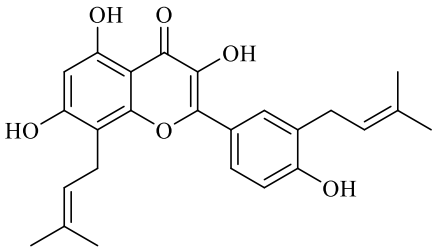
3,5,7-trihydroxy-2-(4-hydroxyphenyl)-6-(3-methyl-2-butenyl)-4H-1-benzopyran-4-one

SF6



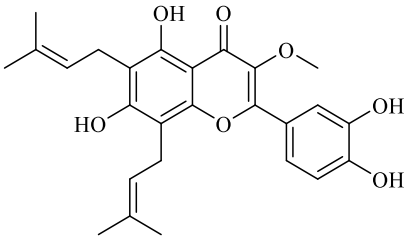
3,5,7-Trihydroxy-2-[4-hydroxy-3-(3-methyl-2-butenyl)phenyl]-4H-1-benzopyran-4-one

SF7



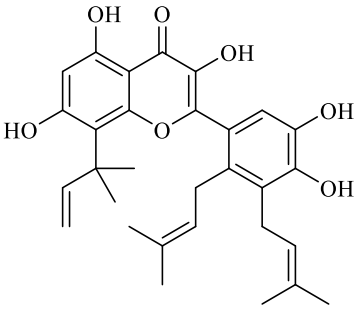
3,5,7-Trihydroxy-2-[4-hydroxy-3-(3-methyl-2-butenyl)phenyl]-8-(3-methyl-2-butenyl)-4H-1-benzopyran-4-one

SF8



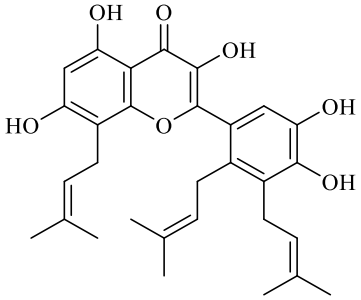
2-(3,4-Dihydroxy-phenyl)-5,7-dihydroxy-3-methoxy-8-((E)-3-methyl-but-2-enyl)-6-(3-methyl-but-2-enyl)-1- benzopyran-4-one

SF9



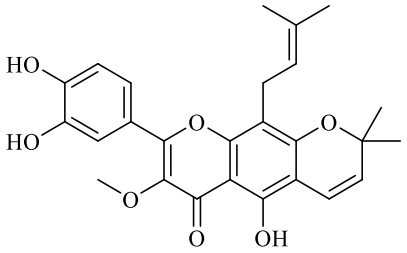
2-(4,5-Dihydroxy-2-(3-methyl-but-2-enyl)-3-((E)-3-methyl-but-2-enyl)-phenyl-8-(1,1-dimethyl-allyl)-3,5,7-trihydroxy-1-benzopyran-4-one

SF10



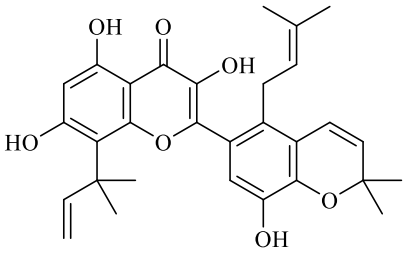
2-(4,5-dihydroxy2-(4,5-dihydroxy-2,3-bis(3-methylbut-2-enyl)phenyl)- 3,5,7-trihydroxy-8-(3- methylbut-2-enyl)chromen-4-one

SF11



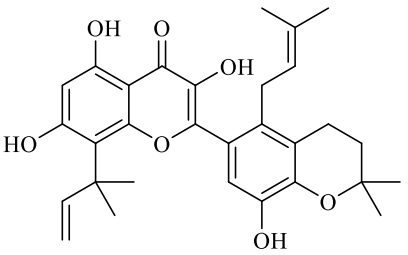
8-(3,4-dihydroxyphenyl)-5-hydroxy-7-methoxy-2,2-dimethyl-10-(3-methylbut-2-en-1-yl)2H,6H-pyrano[3,2-g]chromen-6-one

SF12



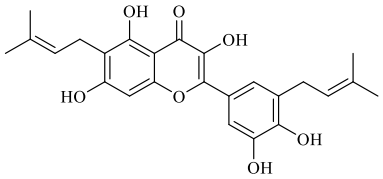
3,5,7-trihydroxy-2-[8-hydroxy-2,2-dimethyl-5-(3-methylbut-2-enyl)chromen-6-yl]-8-(2-methylbut-3-en-2-yl)chromen-4-one

SF13



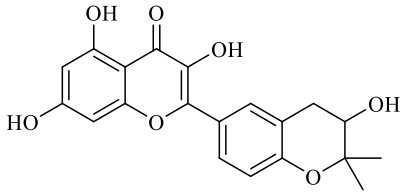
3,5,7-trihydroxy-2-(8-hydroxy-2,2-dimethyl-5-(3-methylbut-2-en-1-yl)chroman-6-yl)-8-(2-methylbut-3-en-2-yl)-4H-chromen-4-one

SF15



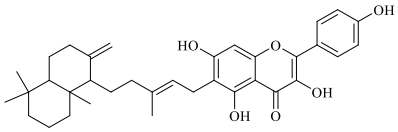
2-(3,4-dihydroxy-5-(3-methylbut-2-en-1-yl)phenyl)-3,5,7-trihydroxy-6-(3-methylbut-2-en-1-yl)-4H-chromen-4-one

SF16



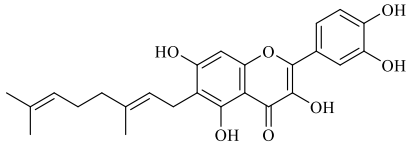
3,5,7-trihydroxy-2-(3-hydroxy-2,2-dimethylchroman-6-yl)-4H-chromen-4-one

17



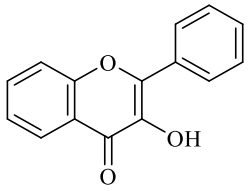
(E)-3,5,7-trihydroxy-2-(4-hydroxyphenyl)-6-(3-methyl-5-(5,5,8a-trimethyl-2-methylenedecahydronaphthalen-1-yl)pent-2-en-1-yl)-4H-chromen-4-one

SF20



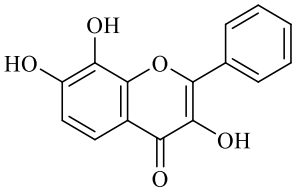
(E)-2-(3,4-dihydroxyphenyl)-6-(3,7-dimethylocta-2,6-dien-1-yl)-3,5,7-trihydroxy-4H-chromen-4-one

SF22



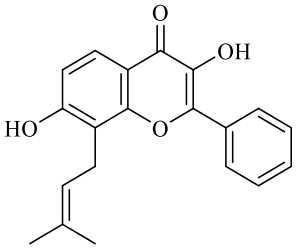
3-hydroxy-2-phenyl-4H-chromen-4-one

SF23



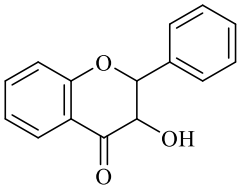
3,7,8-trihydroxy-2-phenyl-4H-chromen-4-one

SF24



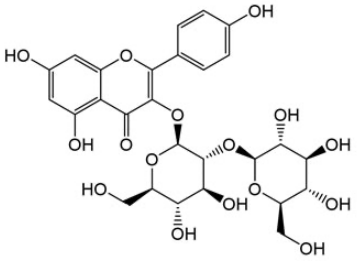
3,7-dihydroxy-8-(3-methylbut-2-en-1-yl)-2-phenyl-4H-chromen-4-one

SF25

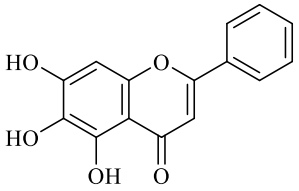


3-hydroxy-2-phenylchroman-4-one

SF14



Kaempferol 3-O-sophoroside



Baicalein (control Positive)
5,6,7-trihydroxy-2-phenyl-4H-chromen-4-one

Fig. 1. Chemical structures of representative flavonol compounds.

The drug-likeness of the 25 flavonol compounds was evaluated using SwissADME based on Lipinski's Rule of Five. The predefined physicochemical criteria considered molecular weight, lipophilicity (logP), hydrogen-bond donors, and hydrogen-bond acceptors. In accordance with the screening strategy used in this study, a maximum of one violation of the predefined criteria was allowed for a

compound to be retained for subsequent analysis. Compounds showing more than one violation were excluded from further analysis. The number and type of violations for each compound were recorded and are presented in Table 1. The rotatable-bond count was also reported as an additional drug-likeness descriptor but was not considered an independent Lipinski Rule-of-Five violation.

2.4 Target prediction and network analysis

The potential molecular targets of the selected flavonols were predicted using SwissTargetPrediction (restricted to *Homo sapiens*). To identify targets relevant to COVID-19, a complementary search was performed using GeneCards. The overlap between the predicted flavonol targets and COVID-19–associated proteins was visualized using a Venn diagram, and the intersecting proteins were further examined in STRING-DB [19] to construct protein–protein interaction (PPI) networks, i.e., maps showing which proteins are known or predicted to physically or functionally interact with one another, used here to identify the proteins that occupy the most central, highly connected positions within the network. Pathway enrichment analysis of the hub proteins was performed in STRING-DB using a hypergeometric test against the KEGG and Gene Ontology (Biological Process) annotation sets, with Benjamini–Hochberg correction applied to control the false discovery rate (FDR); enriched terms with FDR-adjusted $p < 0.05$ were considered statistically significant.

2.5 Molecular docking

Docking experiments were performed using MOE 2022.02 software. The structure of ACE2 (PDB ID: 7BZ5) was prepared by removing water molecules and co-crystallized ligands. The binding site was defined using the MOE Site Finder tool, which identified the largest alpha-sphere pocket corresponding to the known extracellular Spike-protein-binding interface of ACE2. This site was centered at point (60, 56, 74) Å, which encompasses the critical residues involved in the interaction with the viral Spike receptor-binding domain. This selection was validated by the reference compound, baicalein, which demonstrated stable binding interactions at this interface, consistent with previous literature documenting its ability to interfere with Spike–ACE2 binding [reference].

3. Results and Discussion

3.1 Compound screening

A total of 25 flavonol compounds were retrieved from the KNApSAcK database and used as the starting dataset for this study, together with baicalein as the positive control (Fig. 1). The dataset comprised linarin, resokaempferol, kaempferol, morin, licoflavonol, isolicoflavonol, broussoflavonol F, broussoflavonol B, broussoflavonol C, broussoflavonol G, broussoflavonol A, broussoflavonol D, broussoflavonol E, kaempferol 3-O-sophoroside, broussonol E, glycyrrhiza flavonol A, denticulaflavonol, 6-hydroxykaempferol 3-rutinoside, pancibiflavonol, 5,7,3',4'-tetrahydroxy-6-geranylflavonol, 5,7,4'-trihydroxy-8-p-hydroxybenzyldihydroflavonol, 3-hydroxyflavone, 7,8-dihydroxyflavonol, maackiaflavonol, and dihydroflavonol. Structurally, all of these compounds share the characteristic 3-hydroxyflavone (flavonol) backbone but differ in the degree and position of hydroxylation, methoxylation, and prenylation. The broussoflavonol series (broussoflavonol A-G) and related compounds such as licoflavonol, isolicoflavonol, and denticulaflavonol carry additional prenyl or geranyl substituents that increase their molecular weight and lipophilicity, whereas compounds such as kaempferol, morin, 3-hydroxyflavone, and dihydroflavonol represent simpler, less-substituted flavonol scaffolds. This structural diversity provided a broad chemical space for evaluating pharmacokinetic suitability and SARS-CoV-2

inhibitory potential in the screening steps described below.

Based on the previously discussed selection criterion, 21 of the 25 compounds were retained, whereas four compounds (SF1, SF14, SF18, and SF19) were excluded because they exhibited three violations involving molecular weight, hydrogen-bond donors, and hydrogen-bond acceptors. Five of the retained compounds (SF9, SF10, SF12, SF13, and SF17) showed a single violation associated with molecular weight, whereas the remaining 16 retained compounds showed no violations of the evaluated Lipinski criteria.

Thus, the 21 retained flavonols were considered to have met the predefined Lipinski-based screening criterion, while not necessarily being strictly compliant with every individual Rule-of-Five threshold. These criteria violations predict poor absorption and limited oral bioavailability though compounds can still be worth further investigation despite falling short here. This distinction provides a more accurate representation of the screening procedure and avoids overinterpretation of Lipinski compliance. The retained compounds were subsequently subjected to target prediction and network pharmacology analysis [12]. This finding suggests that most flavonols possess favorable physicochemical characteristics that allow them to passively cross cell membranes and potentially act as orally available drug candidates [13]. The list of compounds that fulfilled Lipinski's rule of five are presented in Table 1.

Table 1. Drug-likeness and Lipinski-based screening of the 25 flavonol compounds.

Code	Flavonol compounds	Parameter					Lipinski compliant
		Molecular weight (g/mol) **< 500**	LogP **< 5**	Hydrogen bond donor **< 5**	Hydrogen bond acceptor **< 10**	Number of rotatable bonds **< 10**	
SF1	**Linarin**	**592.55**	**-2.76**	**7**	**14**	**7**	**No**
SF2	Resokaempferol	270.24	0.52	3	5	1	Yes
SF3	Kaempferol	286.24	-0.03	4	6	1	Yes
SF4	Morin	302.24	-0.56	5	7	1	Yes
SF5	Licoflavonol	354.35	1.09	4	6	3	Yes
SF6	Isolicoflavonol	354.35	1.09	4	6	3	Yes
SF7	Broussoflavonol F	422.47	2.09	4	6	5	Yes
SF8	Broussoflavonol B	452.50	1.77	4	7	6	Yes
SF9	Broussoflavonol C	506.59	2.48	5	7	7	Yes
SF10	Broussoflavonol G	506.59	2.48	5	7	7	Yes
SF11	Broussoflavonol A	450.48	1.77	3	7	4	Yes
SF12	Broussoflavonol D	504.57	2.48	4	7	5	Yes
SF13	Broussoflavonol E	506.59	2.55	4	7	5	Yes
SF14	**Kaempferol 3-O-sophoroside**	**610.52**	**-4.16**	**10**	**16**	**7**	**No**
SF15	Broussonol E	438.47	1.56	5	7	5	Yes
SF16	Glycyrrhiza flavonol A	370.35	0.36	4	7	1	Yes
SF17	Denticulaflavonol	558.70	4.01	4	6	6	Yes
SF18	**6 Hydroxykaempferol 3-rutinoside**	**610.52**	**-3.89**	**10**	**16**	**6**	**No**
SF19	**Pancibiflavonol**	**572.47**	**-0.57**	**8**	**12**	**3**	**No**
SF20	5,7,3',4'-Tetrahydroxy-6-geranylflavonol	438.47	1.56	5	7	6	Yes
SF21	5,7,4'-Trihydroxy-8-p-hydroxybenzyldihydroflavonol	394.37	0.77	5	7	3	Yes
SF22	3-Hydroxyflavone	238.24	1.66	1	3	1	Yes
SF23	7,8-Dihydroxyflavonol	270.24	0.52	3	5	1	Yes
SF24	Maackiaflavonol	322.35	2.20	3	4	3	Yes
SF25	Dihydroflavonol	240.25	1.58	1	3	1	Yes

Screening of flavonols using Lipinski's Rule of Five provided an important first filter to identify compounds with favorable physicochemical and pharmacokinetic characteristics. Of the 25 flavonols examined, 21 satisfied all four Lipinski parameters, indicating that they are sufficiently small, not overly polar, and balanced in terms of lipophilicity to have the potential for oral bioavailability. The four excluded compounds, linarin, kaempferol 3-O-sophoroside, 6-hydroxykaempferol 3-rutinoside, and pancibiflavonol, shared the common features of having molecular weights above 500 Da and excessive hydrogen bonding groups, both donors and acceptors. These properties are typically associated with poor passive diffusion across intestinal membranes, reduced permeability, and suboptimal absorption. In contrast, compliant compounds possess moderate molecular sizes and logP values that allow them to maintain solubility while remaining lipophilic enough to cross membranes. This supports the broader observation that naturally occurring flavonols with molecular weights under 500 Da are more likely to be orally bioavailable and can serve as attractive lead scaffolds for further optimization.

3.2 Target prediction and network analysis

SwissTargetPrediction was used to identify the possible protein targets. Of the 21 Lipinski-compliant flavonols, 20 were successfully mapped to 251 predicted targets. For each compound, predicted targets were retained for subsequent network analysis. Target predictions from individual flavonols were subsequently combined to generate a non-redundant list of flavonol-associated proteins. When the same protein was predicted for multiple flavonols, it was counted only once in the unique target list but the corresponding compound–target associations were retained to preserve information regarding target overlap. This procedure resulted in 251 unique predicted targets from the 20 compounds, whereas one (SF21) showed no relevant interactions. In parallel, GeneCards analysis identified 16,290 proteins associated with COVID-19 pathology. Fig. 2 illustrates how these two groups of proteins overlap.

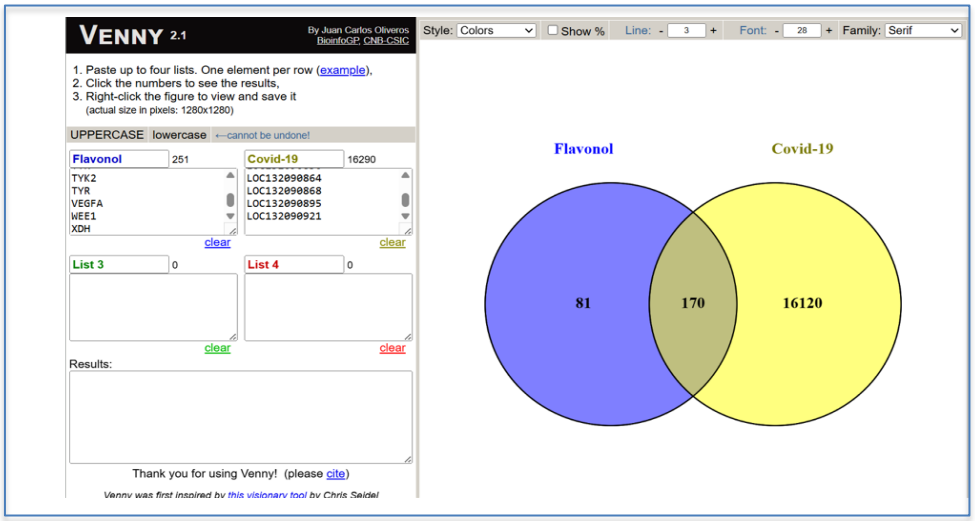


Fig. 2 Venn diagram (purple: Flavonol-associated proteins; yellow: COVID-19–associated proteins; Overlap: Indicates proteins that both interact with flavonol compounds and are involved in COVID-19 pathology).

When both datasets were integrated using a Venn diagram, 170 common proteins were identified as being both flavonol targets and COVID-19–associated proteins. These were further refined using STRING-DB, which revealed 16 central proteins that formed a tightly interconnected protein–protein interaction network (Fig. 3). The 16 hub proteins identified were ACE2, ACE, AGT, REN, TMPRSS2, FURIN, CD4, CD8A, IL6, IL1B, IL10, TNF, IFNG, CRP, CXCL8, and CXCL10, spanning the renin–angiotensin system, viral entry/priming factors, and inflammatory/immune mediators relevant to COVID-19 pathophysiology. Hub status was assigned based on connectivity within the STRING-DB network, i.e., the number of direct interaction edges (node degree) linking each protein to the others in the network; proteins occupying the most highly connected positions were considered hubs. Importantly, ACE2 exhibited the highest degree of connectivity among the 16 hub proteins, consistent with its established role as a viral entry point for SARS-CoV-2.

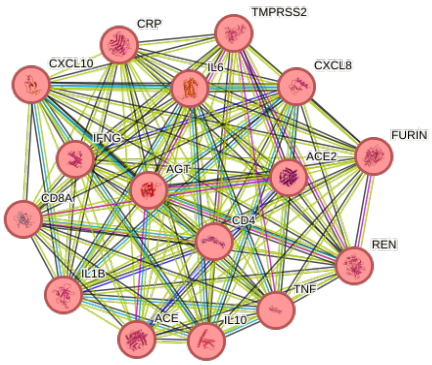


Fig. 3 String DB protein-protein interaction.

The biological significance of the screened flavonols was further explored using a network pharmacology approach, which allowed the integration of chemical-based predictions with disease-related targets. Using SwissTargetPrediction, the potential protein targets of flavonols were computationally mapped based on their structural features and known ligand–protein interactions. In parallel, GeneCards was used to identify proteins associated with COVID-19 pathophysiology, yielding a comprehensive dataset of over 16,000 disease-related proteins. By comparing these two datasets, 170 proteins were identified as overlapping targets, indicating that they were both predicted to interact with flavonols and were known to play a role in COVID-19.

To refine this large set of common proteins into the most relevant candidates, PPI mapping was conducted using the STRING-DB database. This tool analyses protein interactions within biological networks and highlights central “hub” proteins that may exert key regulatory roles. The analysis condensed the 170 overlapping proteins into 16 hub proteins, each occupying a critical position in the COVID-19-related interaction network. These hub proteins represent the points at which flavonol modulation could have the greatest therapeutic impact [19].

Among these 16 hub proteins, ACE, AGT, REN, TMPRSS2, FURIN, CD4, CD8A, IL6, IL1B, IL10, TNF, IFNG, CRP, CXCL8, and CXCL10, ACE2 (angiotensin-converting enzyme 2) emerged as the most highly connected hubs, showing the greatest number of direct interactions (highest node degree) with the other hub proteins in the STRING-DB network. ACE2 is a well-established receptor

for SARS-CoV-2, as the viral spike protein binds directly to ACE2 to facilitate viral entry into host cells. The high connectivity of ACE2 provided a rational basis for selecting it as the representative target for molecular docking. Importantly, the network analysis does not imply that the flavonols have been experimentally demonstrated to bind all 16 hub proteins; rather, it indicates a predicted multitarget relationship at the systems level. The remaining hub proteins represent additional mechanistically relevant targets that warrant target-specific computational and experimental investigation.

The integration of network pharmacology into this study provided a systems-level framework linking flavonols with multiple proteins implicated in COVID-19 pathophysiology. The 16 hub proteins span several biologically relevant processes, including the renin–angiotensin system (ACE2, ACE, AGT, and REN), viral entry and proteolytic activation (ACE2, TMPRSS2, and FURIN), adaptive immune responses (CD4 and CD8A), and inflammatory signaling (IL6, IL1B, IL10, TNF, IFNG, CRP, CXCL8, and CXCL10). Thus, the network analysis supports the proposed multitarget character of the flavonols at the systems level. Because ACE2 had the highest network connectivity, it was selected for molecular docking to provide structural evidence for one representative hub target. However, the present docking analysis does not establish binding to the other 15 hub proteins. Therefore, further molecular docking, molecular dynamics, binding free-energy calculations, and experimental validation involving the remaining hub proteins will be necessary to determine whether the predicted network-level multitarget activity translates into direct target engagement.

3.2.1 Pathway enrichment analysis

To interpret the biological relevance of the 16 hub proteins beyond their network connectivity, KEGG pathway and Gene Ontology (Biological Process) enrichment analyses were performed as described in Section 2.4. Final enrichment results below from the STRING-DB Functional Enrichment output, or DAVID/Enrichr/g:Profiler export, (full gene lists in Supplementary Material) summarizes the most significantly enriched pathways/terms among the 16 hub proteins.

Based on the identity of the 16 hub proteins (ACE2, ACE, AGT, REN, TMPRSS2, FURIN, CD4, CD8A, IL6, IL1B, IL10, TNF, IFNG, CRP, CXCL8, and CXCL10), enriched terms are expected to include the renin–angiotensin system pathway, cytokine–cytokine receptor interaction, and viral entry/proteolytic priming processes; this must be confirmed by the actual enrichment statistics rather than assumed from protein identity alone.

3.3 Molecular docking of positive control

The reference compound, baicalein, exhibited a binding free energy of –5.31 kcal/mol and an RMSD of 1.20 Å, forming hydrogen bonds with Asp467 and Glu471, van der Waals interactions, and hydrophobic contacts with Arg454, Arg457, and Lys458 and additional van der Waals interactions with residues surrounding the ligand. Hydrophobic contacts and van der Waals interactions are reported separately according to the interaction classification generated by the docking software. This served as a benchmark for evaluating the docking performance of testing flavonols. Spatial arrangement of this interaction is depicted in Fig. 4.

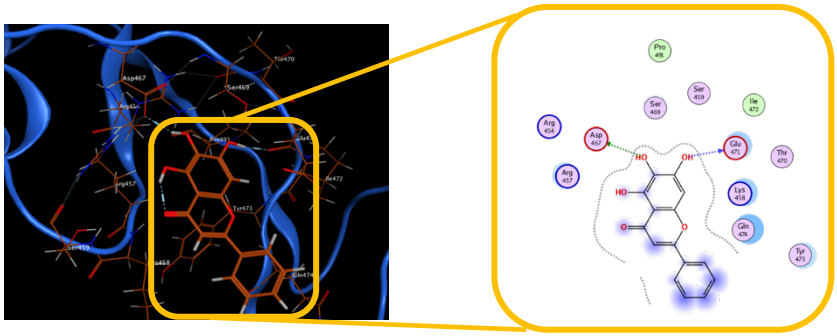


Fig. 4 Molecular interaction diagram of baicalein in the ACE2 binding site. In the interaction analysis, hydrophobic contacts and van der Waals interactions were treated as distinct interaction types. Hydrophobic contacts refer to contacts involving nonpolar regions of the ligand and protein residues, whereas van der Waals interactions represent short-range nonbonded contacts. These interaction types were therefore described in the text rather than distinguished by additional graphical modifications to the Fig. 4.

Baicalein was chosen as a reference compound in this study because its antiviral activity against SARS-CoV-2 has been reported in both experimental and computational investigations, making it a reliable positive control for the docking analysis [22, 23]. In silico docking simulations revealed that baicalein could bind to the ACE2 receptor with a free binding energy of –5.31 kcal/mol. This negative binding energy indicates that the interaction is thermodynamically favorable, and the magnitude of the value suggests a moderately strong affinity between baicalein and ACE2 [22, 23].

3.4 Molecular docking of flavonol derivatives

Docking of the 20 flavonols against ACE2 showed that all six compounds listed in Table 2 (Isolicoflavonol, Broussoflavonol B, Broussoflavonol A, Broussonol E, Glycyrrhiza flavonol A, and 5,7,3′,4′-tetrahydroxy-6-geranylflavonol) exhibited stronger binding affinities than baicalein, with binding free energies ranging from –6.02 to –6.95 kcal/mol compared to –5.31 kcal/mol for baicalein. Results for molecular docking are presented in Table 2. Applying the docking-score-based criterion defined in Section 2.5, the four top hits were Broussonol E, 5,7,3′,4′-tetrahydroxy-6-geranylflavonol, Broussoflavonol A, and Broussoflavonol B, with binding free energies ranging between –6.35 and –6.95 kcal/mol. These four compounds also exhibited low RMSD values (1.09–1.34 Å), indicating reliable, reproducible docking poses.

The residues identified in our interaction profile, specifically Arg454, Arg457, Lys458, Asp467, and Glu471, are localized to the ACE2 N-terminal peptidase domain, which constitutes the primary interface for SARS-CoV-2 Spike protein binding. The consistent interaction of our top flavonol hits with these residues, particularly the hydrogen bonding with Asp467 and Glu471 and hydrophobic contacts with Arg454, Arg457, and Lys458, suggests that these compounds bind at the precise site where the viral receptor-binding domain normally docks. This spatial alignment supports the proposed mechanism of competitively inhibiting the Spike–ACE2 interaction.

Table 2. Docking Results.

Compound	Parameter						
	S (kcal/mol)	RMSD	Hydrogen bond	Hydrophobic	Van der Waals	Other interaction	Binding Factor
Baicalein (positive control)	-5.3109	1.1980	Asp467 Glu471	Arg454 Arg457 Lys458	Asp467 Glu471	Pro491 Ser469 Ser459 Ile472 Tyr473 Thr470 Gln474 Phe456	12
SF2 (Pose 9)	-4.7578	1.3898	Asp467	Arg454 Arg457 Lys458	Asp467 Glu471	Pro491 Ser469 Ile472 Tyr473 Gln474	10
SF3 (Pose 11)	-5.6447	1.4186	Asp467 Glu471 Lys458	Arg454 Arg457 Lys458	Glu471 Asp467	Pro491 Ser469 Ser459 Tyr473 Thr470 Gln474	11
SF4 (Pose 22)	-5.5099	1.0730	Asp467 Lys458	Arg454 Arg457 Lys458	Glu471 Asp467	Pro491 Ser469 Ser459 Tyr473 Thr470 Gln474	11
SF5 (Pose 35)	-5.7519	1.1617	-	Arg454 Arg457 Lys458	Glu471 Asp467	Pro491 Pro479 Ser459 Tyr473 Gln474 Ile472 Asn481 Cys480	10
SF6 (Pose 45)	-6.0218	1.0084	Glu471 Gln474	Arg454 Arg457 Lys458	Glu471 Asp467	Pro491 Ser469 Ser459 Tyr473 Gln474 Ile472	11
SF7 (Pose 60)	-5.7409	1.7940	Asp 467	Arg 454 Arg 457 Lys 458	Glu 471 Asp 467	Phe 456 Pro 491 Ser 469 Ile 472 Tyr 473 Gln 474	10
SF8 (Pose 61)	-6.3462	1.1311	Ser469 Phe456	Arg454 Arg457 Lys458	Glu471	Pro491 Ile472 Tyr473 Thr470 Ser459 Gln474	11
SF9 (Pose 73)	-6.3337	1.3767	Asp467 Gln474	Arg454 Arg457 Lys458	Glu471 Asp467	Pro491 Ser459 Ser469 Ile472 Tyr473 Gln474	11
SF10 (Pose 83)	-6.3748	1.4847	Ile472	Arg454 Arg457 Arg466	Glu465 Glu471 Asp467	Pro491 Ser459 Ser469	11

				Lys458		Tyr473 Gln474 Phe456 Pro491 Ser459 Ser469	
SF11 (Pose 91)	-6.5226	1.2410	Asp467	Arg454 Arg457 Lys458	Glu471 Asp467	Ile472 Gln474 Tyr473 Phe456 Gly476 Pro491	11
SF12 (Pose 108)	-6.2173	1.3285	Asp467	Arg454 Arg457 Lys458	Glu471 Asp467	Ser459 Ser469 Ile472 Gln474 Tyr473 Pro491	11
SF13 (Pose 118)	-6.2467	0.8835	Asp467	Arg454 Arg457 Lys458	Glu471 Asp467	Ser459 Ser469 Ile472 Gln474 Tyr473 Gly476	11
SF15 (Pose 121)	-6.9528	1.3369	Glu471	Arg454 Arg457 Lys458	Glu471 Asp467	Ser469 Ile472 Pro491 Tyr473 Gln474 Asn481	10
SF16 (Pose 134)	-6.2666	1.1608	Glu471 Gln474	Arg454 Arg457 Lys458	Glu471 Asp467	Cys480 Gly482 Pro479 Phe456 Phe456 Ile472 Pro491 Thr470 Ser469 Tyr473	11
SF17 (Pose 149)	-6.3084	1.7951	Glu471	Arg454 Arg457 Lys458	Glu471 Asp467	Gln474 Gly476 Phe456 Pro491 Tyr473 Ser459 Ser469 Gln474 Ile472 Asn481 Gly482	11
SF20 (Pose 154)	-6.6069	1.0901	Glu465 Ser459	Arg454 Arg457 Lys458 Lys462	Glu471 Asp467 Glu465	Cys480 Ser469 Tyr473 Gln474 Ile472 Pro491 Phe456 Ser469	11
SF22 (Pose 161)	-4.9342	2.0352	Lys458	Arg454 Arg457 Lys458	Glu471 Asp467	Ser459 Tyr473 Pro491 Ile472 Gln474	11
SF23 (Pose 171)	-5.3151	0.9863	Asp467 Gln474	Arg454 Arg457	Glu471 Asp467	Ser459 Ser469	10

				Lys458		Ile472 Gln474 Tyr473 Ser459 Ser469	
SF24 (Pose 183)	-5.3512	1.0828	Asp467 Gln474	Arg454 Arg457 Lys458	Glu471 Asp467	Ile472 Gln474 Tyr473	10
SF25 (Pose 191)	-4.9906	1.0909	Gln474 Ile472	Arg454 Arg457 Lys458	Glu471 Asp467	Tyr473 Ser469	9

The stability of this binding was further supported by the interaction profile. Baicalein formed hydrogen bonds with Asp467 and Glu471, two amino acid residues located within the ACE2 binding pocket. Hydrogen bonds play a key role in orienting ligands and stabilizing their conformations within the protein active site. In addition, hydrophobic contacts with Arg454, Arg457, and Lys458 contributed to the overall stabilization of the ligand–receptor complex by reinforcing the nonpolar interactions within the pocket. The combination of hydrogen bonding and hydrophobic contacts mirrors the types of interactions typically observed in effective inhibitors, strengthening the confidence that baicalein interacts in a biologically meaningful way with ACE2.

These computational findings align well with published experimental data, which show that baicalein inhibits viral entry by interfering with the spike protein–ACE2 interaction. Previous docking studies have also reported similar residue-level interactions between baicalein and ACE2, further validating the accuracy of the docking results obtained in this study [reference]. The consistency between the in silico predictions and in vitro findings enhances the reliability of the docking workflow used in this study.

By including baicalein as a positive control, this study established a comparative standard against which flavonol derivatives could be evaluated. Since the activity of baicalein has been experimentally verified, any compound showing a stronger binding affinity or comparable interaction patterns can be considered a promising lead with potentially greater antiviral potential. Thus, baicalein served as a validation tool for the docking protocol and as a critical benchmark for interpreting the relative performance of the test flavonols in binding to ACE2 [17].

Interestingly, these four flavonols shared 11 overlapping amino acid interactions with baicalein, suggesting that they occupy the ACE2 binding site in a highly similar manner. This overlap highlights their potential to interfere with the same protein regions targeted by reference compounds. Spatial arrangement of these compounds with protein are presented in Fig. 5.

Among the docked flavonols, the four defined top hits Broussonol E, 5,7,3′,4′-tetrahydroxy-6-geranylflavonol, Brousso-flavonol A, and Broussoflavonol B emerged as the most promising candidates, all demonstrating stronger binding affinities than baicalein, with docking scores ranging from –6.35 to –6.95 kcal/mol. They also displayed reliable RMSD values (1.09–1.34 Å), reflecting stable, reproducible binding poses, and showed substantial overlap in the ACE2 residues contacted by baicalein (e.g., Asp467, Glu471), suggesting a similar occupation of the binding site. Of these, Broussonol E and 5,7,3′,4′-tetrahydroxy-6-geranylflavonol showed the strongest binding, with the geranyl and additional hydroxyl substituents on these scaffolds potentially contributing extra hydrophobic and hydrogen-bonding contacts within the ACE2 pocket [AUTHORS: please confirm/refine this structural rationale against your docking poses]. This observation is broadly consistent with previous studies reporting that additional hydroxyl and prenyl/geranyl substitutions in flavonols can improve binding and antiviral activity.

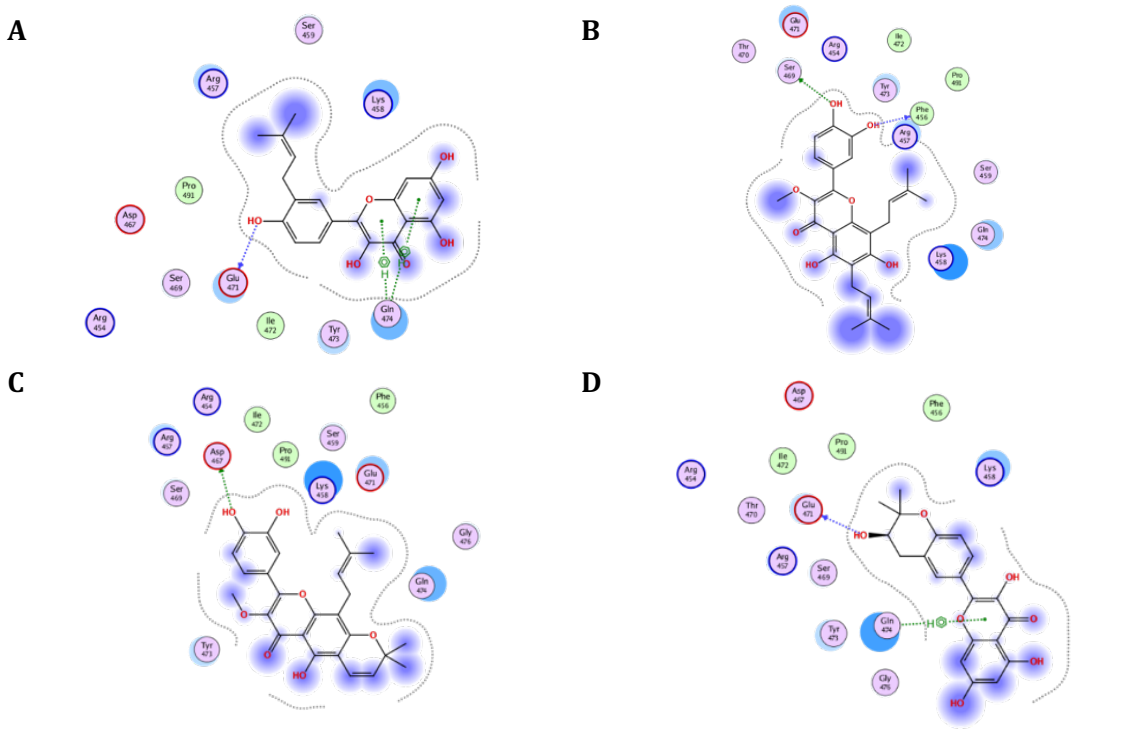


Fig. 5. Spatial arrangement of (a) Isolicoflavonol (SF6), (b) Broussoflavonol B (SF8), (c) Broussoflavonol A (SF11), and (d) Glycyrrhiza flavonol A (SF16) with protein
Note: Dotted lines indicated hydrogen bonding.
: hydrophobic interaction : van der Waals interaction

Superimposition of the four top hits Broussonol E, 5,7,3′,4′-tetrahydroxy-6-geranylflavonol, Broussoflavonol A, and Broussoflavonol B with baicalein further confirmed that these compounds adopted similar orientations within the ACE2 binding pocket. The key difference lies in the ability of Broussonol E and 5,7,3′,4′-tetrahydroxy-6-geranylflavonol to establish additional/alternative hydrogen-bonding and hydrophobic contacts.

While our findings highlight the therapeutic potential of flavonols in disrupting the Spike–ACE2 interaction, it is crucial to acknowledge that ACE2 is a key host enzyme within the renin–angiotensin system, essential for maintaining blood pressure and cardiovascular homeostasis. Consequently, pharmacological modulation of ACE2 presents potential biological and safety risks, including the possibility of unintended hypertensive or inflammatory effects if ACE2 activity is significantly impaired. Therefore, the computational results presented here are intended as a preliminary screen for potential lead scaffolds. Further studies, including cell-based safety assays and detailed in vitro functional testing, are imperative to assess the physiological impact of these flavonols on native ACE2 function before they can be considered for therapeutic development. While static docking provides valuable structural insight into binding modes and residue-level contacts at the ACE2 interface, it does not capture conformational transitions, solvent dynamics, or the time-dependent stabilization of the protein upon ligand binding. Comprehensive molecular dynamics simulations of the apo-protein and protein–inhibitor complexes, alongside binding free energy calculations (e.g., MM-PBSA/GBSA) and experimental enzyme kinetics, will be necessary in future work to

fully characterize the dynamic stability and inhibitory mechanisms of these top hits.

4. Conclusion

This study applied an integrated network pharmacology and molecular docking approach to evaluate flavonols as potential multitarget antiviral candidates against COVID-19. In total, 25 flavonols were screened, 21 satisfied Lipinski's Rule of Five, indicating favorable drug-like properties. Network analysis identified 170 proteins common to flavonol-associated targets and COVID-19-related proteins, highlighting 16 highly connected hub proteins (ACE2, ACE, AGT, REN, TMPRSS2, FURIN, CD4, CD8A, IL6, IL1B, IL10, TNF, IFNG, CRP, CXCL8, and CXCL10) consistent with a multitarget mode of action. ACE2, the most highly connected hub, was selected as a representative target for molecular docking, and four flavonols—Broussonol E, 5,7,3′,4′-tetrahydroxy-6-geranylflavonol, Broussoflavonol A, and Broussoflavonol B—achieved the most favorable docking scores (−6.35 to −6.95 kcal/mol), each outperforming the reference compound baicalein (−5.31 kcal/mol) and sharing several interaction residues with it. However, direct interactions with the remaining 15 hub proteins were not evaluated by docking and should not be considered confirmed. Further, the docking scores and RMSD values reported are static, pose-based metrics that do not by themselves establish dynamic complex stability or true binding free energy; molecular dynamics simulations with MM-GBSA/MM-PBSA analysis and in vitro functional assays are therefore needed to determine whether the predicted multitarget activity translates into measurable antiviral effects.

References

[1] Huang Y, Yang C, Xu XF, Xu W, Liu SW. Structural and functional properties of SARS-CoV-2 spike protein: potential antivirus drug development for COVID-19. Acta Pharmacol Sin. 2020 Sep;41(9):1141-9.

[2] Chugh H, Awasthi A, Agarwal Y, Gaur RK, Dhawan G, Chandra R. A comprehensive review on potential therapeutics interventions for COVID-19. Eur J Pharmacol. 2021 Jan 5;890:173741.

[3] Karak, P. 2019. Biological Activities of Flavonoids: an Overview. *Int. J. Pharm. Sci. Res*, 10(4): 1567–74.

[4] Boukhatem, M.N. & Setzer, W.N. 2020. Aromatic Herbs, Medicinal Plant-Derived Essential Oils, and Phytochemical Extracts as Potential Therapies for Coronaviruses: Future Perspectives. *Plants*, 9(6): 1–23.

[5] Lalani, S. & Poh, C.L. 2020. Flavonoids as Antiviral Agents for Enterovirus A71 (EV-A71). *Viruses*, 12(2): 184.

[6] Panche 2016. Flavonoids: an Overview. *J. Nutr. Sci*, 5(47): 1–5.

[7] Chaves, O.A., Fintelman-Rodrigues, N., Wang, X., Sacramento, C.Q., Temerozo, J.R., Ferreira, A.C., Mattos, M., Pereira-Dutra, F., Bozza, P.T., Castro-Faria-neto, H.C., Russo, J.J., Ju, J. & Souza, T.M.L. 2022. Commercially Available Flavonols Are Better SARS-CoV-2 Inhibitors Than Isoflavone and Flavones. Viruses, 14(7): 1458.

[8] Roy, A. V., Chan, M., Banadyga, L., He, S., Zhu, W., Chrétien, M. & Mbikay, M. 2024. Quercetin Inhibits SARS-CoV-2 Infection and Prevents Syncytium Formation by Cells Co-Expressing the Viral Spike Protein and Human ACE2. *Virology Journal*, 21(1): 29.

[9] Fath, D.H.M., Muchlisin, M.A. & Jamil, A.S. 2024. Analisis Network Pharmacology Senyawa Metabolit Sekunder Tanaman Lengkuas (Alpinia galanga) pada Penyakit Kanker. *Journal of Islamic Pharmacy*, 9(1): 43–9.

[10] Wu, L., Chen, Y., Yi, J., Zhuang, Y., Cui, L. & Ye, C. 2020a. Mechanism of Action of Bu-Fei-Yi-Shen Formula in Treating Chronic Obstructive Pulmonary Disease Based on Network Pharmacology Analysis

and Molecular Docking Validation. *BioMed Research International*, 2020(1): 9105972.

[11] Daina, A., Michielin, O. & Zoete, V. 2019. SwissTargetPrediction: Updated Data and New Features for Efficient Prediction of Protein Targets of Small Molecules. *Nucleic Acids Research*, 47(1): 357–64.

[12] Chagas, C.M., Moss, S. & Alisaraie, L. 2018. Drug Metabolites and Their Effects on the Development of Adverse Reactions: Revisiting Lipinski's Rule of Five. *International Journal of Pharmaceutics*, 549(1–2): 133–49.

[13] Sahlan, M., Irdiani, R., Flamandita, D., Aditama, R., Alfarraj, S., Ansari, M.J., Khayrani, A.C., Pratami, D.K. & Lischer, K. 2021. Molecular Interaction Analysis of Sulawesi Propolis Compounds with SARS-CoV-2 Main Protease as Preliminary Study for COVID-19 Drug Discovery. *Journal of King Saud University - Science*, 33(1): 101234.

[14] Nakamura, Y., Mochamad Afendi, F., Kawsar Parvin, A., Ono, N., Tanaka, K., Hirai Morita, A., Sato, T., Sugiura, T., Altaf-Ul-Amin, M. & Kanaya, S. 2014. KNApSAcK Metabolite Activity Database for Retrieving the Relationships Between Metabolites and Biological Activities. *Plant and Cell Physiology*, 55(1): 1–9.

[15] Hoffmann, M., Kleine-Weber, H., Schroeder, S., Krüger, N., Herrler, T., Erichsen, S., Schiergens, T.S., Herrler, G., Wu, N.H., Nitsche, A., Müller, M.A., Drosten, C. & Pöhlmann, S. 2020. SARS-CoV-2 Cell Entry Depends on ACE2 and TMPRSS2 and Is Blocked by a Clinically Proven Protease Inhibitor. *Cell*, 181(2): 271–80.

[16] Frimayanti, N., Ikhtiarudin, I., Ardiyansyah, R. *et al.* 2025. Design and in Silico evaluation of 3',4'-Dimethoxy flavonol as promising SARS-CoV-2 main protease (M^{pro}) inhibitor. *In Silico Pharmacol.* 13:78.

[17] Mouffouk, C., Mouffouk, S., Mouffouk, S., Hambaba, L. & Haba, H. 2021. Flavonols as Potential Antiviral Drugs Targeting SARS-CoV-2 Proteases (3CLpro and PLpro), Spike Protein, RNA-Dependent RNA Polymerase (RdRp) and Angiotensin-Converting Enzyme II Receptor (ACE2). *European Journal of Pharmacology*, 891: 891–173759.

[18] Monika, G., Punam, G., Sarbjot, S. & D, G.G. 2016. An Overview on Molecular Docking. *Journal of Drug Development and Research*, 2(2): 219–31.

[19] Szklarczyk, D., Kirsch, R., Koutrouli, M., Nastou, K., Mehryary, F., Hachilif, R., Gable, A.L., Fang, T., Doncheva, N.T., Pyysalo, S., Bork, P., Jensen, L.J. & von Mering, C. 2023. The STRING Database in 2023: Protein–Protein Association Networks and Functional Enrichment Analyses for Any Sequenced Genome of Interest. *Nucleic Acids Research*, 51(D1): 638–46.

[20] Wu, Y., Wang, F., Shen, C., Peng, W., Li, D., Zhao, C., Li, Z., Li, S., Bi, Y., Yang, Y., Gong, Y., Xiao, H., Fan, Z., Tan, S., Wu, G., Tan, W., Lu, X., Fan, C., Wang, Q., Liu, Y., Zhang, C., Qi, J., Gao, G.F., Gao, F. & Liu, L. 2020. A Noncompeting Pair of Human Neutralizing Antibodies Block COVID-19 Virus Binding to Its Receptor ACE2. *Science*, 368(6496): 1274–8.

[21] Lipinski, C.A., Lombardo, F., Dominy, B.W. & Feeney, P.J. 2001. Experimental and Computational Approaches to Estimate Solubility and Permeability in Drug Discovery and Development Settings. *Advanced Drug Delivery Reviews*, 46(1–3): 3–26.

[22] Lin, C.-H., Chang, H.-J., Lin, M.-W., Yang, X.-R., Lee, C.-H. & Lin, C.-S. 2024. Inhibitory Efficacy of Main Components of Scutellaria baicalensis on the Interaction between Spike Protein of SARS-CoV-2 and Human Angiotensin-Converting Enzyme II. *International Journal of Molecular Sciences*, 25(5): 2935.

[23] Lin, C.H., Lin, M.W., Chiang, H.H., Wu, T.H., Tsai, C.H. & Lin, C.S. 2025. Comprehensive Insights into the Therapeutic Effects of Baicalein and Baicalin against SARS-CoV-2 Infection. *Phytomedicine Plus*, 5(3): 100851.